

Carrier-mediated ferromagnetic ordering in Mn ion-implanted p^+ GaAs:CY. D. Park^{1,*} J. D. Lim,² K. S. Suh,¹ S. B. Shim,¹ J. S. Lee,² C. R. Abernathy,³ S. J. Pearton,³ Y. S. Kim,² Z. G. Khim,² and R. G. Wilson⁴¹*CSCMR and School of Physics, Seoul National University, Seoul 151-747 Korea*²*School of Physics, Seoul National University, Seoul 151-747 Korea*³*Department of Materials Science and Engineering, University of Florida, Gainesville, Florida 32605, USA*⁴*Stevenson Ranch, California 91381, USA*

(Received 7 March 2003; revised manuscript received 17 April 2003; published 29 August 2003)

Highly p -type GaAs:C was ion implanted with Mn at differing doses to produce Mn concentrations in the 1–5 at. % range. In comparison to LT-GaAs and n^+ GaAs:Si samples implanted under the same conditions, transport and magnetic properties show marked differences. Transport measurements show anomalies, consistent with observed magnetic properties and with epi-LT-(Ga,Mn)As, as well as the extraordinary Hall effect up to the observed magnetic ordering temperature (T_C). Mn ion-implanted p^+ GaAs:C with as-grown carrier concentrations $>10^{20}$ cm⁻³ show remanent magnetization up to 280 K.

DOI: 10.1103/PhysRevB.68.085210

PACS number(s): 61.72.Vv, 75.50.Pp, 75.70.-i

Observation of ferromagnetic ordering in highly Mn doped InAs (Ref. 1) and GaAs (Ref. 2) has spurred renewed interest in diluted magnetic semiconductor (DMS) systems for the possible realization of spintronic devices, ideally requiring a material system with spin-polarized carriers compatible with existing semiconductor electronics.³ Since the original reports of magnetic ordering temperature (T_C) of 110 K for low-temperature (LT) molecular beam epitaxy (MBE) prepared (Ga,Mn)As, researchers elsewhere have reported increases in T_C through optimization of growth conditions and annealing processes.^{4–6} Yet, for realization of practical devices, a material with T_C near or above room temperature would be desirable. From theoretical treatment and experimental evidence, carrier concentration (p) plays an important role in mediating ferromagnetic ordering between localized spins of Mn impurities in the GaAs matrix.^{7–10} Although measurement of p from Hall effect measurements is complicated by the intrinsic extraordinary Hall effect (EHE),¹¹ p measured is far below that of expected if all Mn acceptors are electrically active (p as low as 15–30% of incorporated Mn). Accordingly, only a fraction (as low as 1/7 of Mn reported by Ohldag *et al.* from MCD studies¹²) of the Mn impurities are experimentally observed to participate magnetically. It is widely thought that due to the low temperature (<300 °C) of the substrate during growth, total free p is compensated by deep-level donor defects such as As antisite (As_{Ga}).

The importance of free hole carrier concentration (p) has been demonstrated experimentally by codoping Sn, a donor impurity, and Mn in GaAs during growth.¹³ As free hole carriers are compensated, Satoh *et al.* observed a directly related decrease in T_C . Other than codoping, modulations of carriers by electric field directly correlate to an increase and decrease in T_C in (In,Mn)As (Ref. 14) and MnGe (Ref. 15). Recent experiments in post-growth thermal treatments showed markedly higher T_C 's, which increase is thought to be related to an increase in p by decreasing the number of deep level donor defects, as well as increase in Mn_{Ga} .^{4–6} In theoretical treatments of ferromagnetic ordering in III-Mn-As, it is thought that an increase in p may directly corre-

spond to an increase in T_C up to and beyond room temperature.¹⁰ Here, we present structural, magnetic, and transport properties of high carbon doped GaAs (p^+ GaAs:C) ion implanted with Mn. High carbon doping concentration has been well studied for the development of the base region in high speed heterojunction bipolar transistors (HBT's).¹⁶ Under some growth conditions, it is energetically favorable for carbon to occupy the arsenic site (whereas Mn is known to occupy the Ga site) where it acts as a shallow acceptor with nearly all of the carbon activated.¹⁷ Due to a low diffusion coefficient of carbon in GaAs,¹⁸ carbon concentrations greater than 10^{21} cm⁻³ have been reported, nearly an order of magnitude higher than p reported in LT-(Ga,Mn)As. Carbon ionization energy in GaAs ($E_A - E_v$) is nearly half of that of Mn, possibly allowing to independently control carrier and magnetic impurity concentrations and to investigate conditions where p exceeds the magnetic impurity concentration, not possible in LT-(Ga,Mn)As.

Epitaxial p^+ GaAs:C [$p \sim 3 \times 10^{20}$ cm⁻³ ($\sim 1.4\%$ C_{As}), 500 nm thick] films were grown on semi-insulating (SI) GaAs by gas source molecular beam epitaxy (GSMBE).¹⁹ Under these conditions, codoping of Mn without significant formation of intermetallic clusters would be difficult. Introduction of dopants physically by means of ion-implantation has been well studied to survey various semiconductors and oxides for DMS,²⁰ and recently Scarpulla *et al.* report of single phase (Ga,Mn)As from Mn ion implantation and subsequent pulsed-laser melting of SI GaAs with $T_C \sim 80$ K.²¹ Ion implantation is capable of introducing dopant concentrations above the usual equilibrium solid solubility limit. Thus after growth, samples were ion implanted with Mn at 250 keV with the sample held at ~ 350 °C to minimize amorphization and with Mn doses of 1, 2, 3, 5×10^{16} cm⁻² (samples A, B, C, D, respectively), which corresponds to nearly 1–5 atm.% of Mn. For comparison, LT-MBE prepared GaAs (LT-GaAs) and high Si doped GaAs (n^+ GaAs:Si) epilayers were implanted under the same conditions with Mn dose of 3×10^{16} cm⁻² (samples X, Y). Details of the implantation process are given elsewhere.²⁰ To

further minimize formation of known secondary phases of Ga, Mn, and As, no post implant anneal was performed.

After ion implantation, depth profile auger electron spectroscopy (AES) measurements show Mn to be present down to 300 nm below the surface and consistent with doping profiles found in previous studies.²⁰ To study possible segregation of implanted species at the surface, electron microprobe x-ray analysis (EMPA-JEOL JXA-8900R) indicate a homogeneous surface within resolution of the instrument. High resolution x-ray diffraction (HRXRD) measurements of as-grown and as-implanted samples show similar results, with identifiable peaks that can be only associated to the epilayer and substrate. The resulting implanted samples HRXRD measurements do not show possible secondary phases (such as MnAs and GaMn) or trends as studied by Moreno *et al.* [by annealing LT-(Ga,Mn)As].²² In addition to HRXRD, high resolution cross-sectional transmission electron microscopy (HRXTEM) were performed on samples A and D, but due to the expected high concentrations of structural dislocations, neither qualitative nor quantitative analysis of secondary precipitates was possible.

In previous studies of DMS, physical characterization methods such as HRXRD and HRXTEM as well as others by themselves cannot completely rule out the presence of secondary phases. Transport properties, particularly EHE and anomalies near T_C , as well as magnetic properties may be more sensitive and informative concerning existence of secondary ferromagnetic phases. Hayashi *et al.* in reporting increase in T_C after thermal treatment of as-grown (Ga,Mn)As found that even as-grown samples (with $T_C \sim 40$ K) show a characteristic “hump” in the resistivity as a function of temperature plots.⁴ Akinaga *et al.* in studying nanomagnetic MnAs clusters embedded in GaAs report of characteristic changes in the slope of resistivity as a function of temperature curve around 50 K, independent of whether clusters are formed, and assigned the anomaly to a Ga-Mn-As complex in the matrix.²³ Standard four point probe dc transport measurements from 10 to 300 K were performed using In soldered contacts in a closed-cycle Dewar [Fig. 1(a)]. Remarkably, the Mn implanted p^+ GaAs:C samples show a similar features to LT-MBE prepared (Ga,Mn)As samples. Although a full metal-to-insulator transition was not observed in all implanted samples, it is surprising that such features are distinct given the expectation that the transport properties would be dominated by damage incurred during the implantation process.

For comparison, as-grown p^+ GaAs:C shows metalliclike behavior with no distinct features; while samples X and Y show expected (insulator-like) behavior due to implantation damage. Similar insulatorlike behavior was observed for Co, Cr, and V implanted samples into p^+ GaAs:C [Fig. 1(b)]. ac transport measurements using Quantum Design Physical Property Measurement System (PPMS) (excitation current of 100 μ A at 17.1 Hz) for the temperature range considered (5–300 K) and applied magnetic fields up to 5 T indicate positive magnetoresistance (MR). In granular hybrid systems where nanosized transition metal based ferromagnetic intermetallics are embedded in a semiconductor matrix such as MnAs:GaAs (Ref. 23), ErAs:GaAs (Ref. 24), and

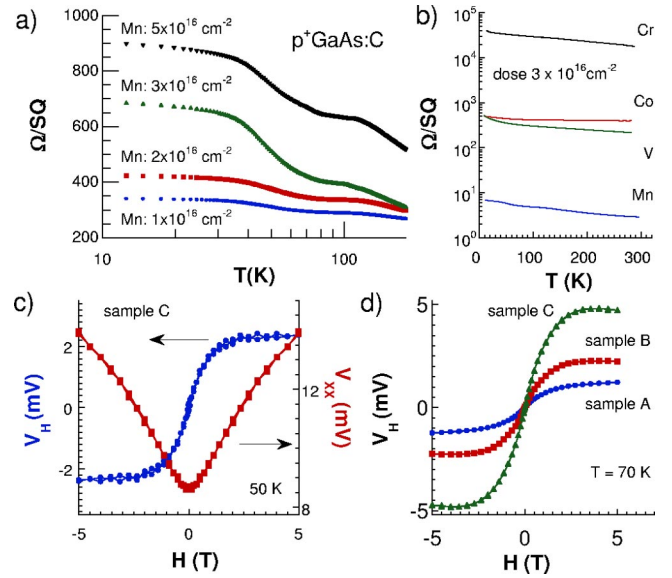


FIG. 1. (Color online) (a) Sheet resistance (Ω/SQ) as function of temperature (T) for samples A–D. (b) Ω/SQ as function of T for Co, Cr, Mn, V implanted p^+ GaAs:C with $3 \times 10^{16} \text{ cm}^{-2}$ dose. (c) ac magneto-transport measurement of sample C at 50 K with excitation current of 100 μ A. (d) ac Hall effect measurement of samples A–C at 70 K.

Mn₁₁Ge₈:Ge (Ref. 25), a crossover in sign of MR from positive at higher temperatures to negative at lower temperatures was observed and attributed to variable hopping mechanisms. Although LT-(Ga,Mn)As show similar behaviors below T_C with a pronounced background negative MR, a positive near parabolic MR behavior around $H=0$ appears for metallic samples below $\sim T_C$.²⁶

Magnetotransport measurements were carried out to estimate sheet carrier concentration (p_s) and determine sheet resistance (Ω/SQ) using the Van der Pauw geometry. General trend shows implanted species to enter the GaAs matrix with an accompanying increase in p_s ($p_s = 1.6 \times 10^{16} \text{ cm}^{-2}$ for sample A to $p_s = 1.1 \times 10^{17} \text{ cm}^{-2}$ for sample D at 300 K), and direct correlation to dose and Ω/SQ due to implantation damage. For example, Cr is a known deep-level donor in GaAs. From Hall measurements, we found the p^+ GaAs:C Cr ion-implanted sample to be fully compensated and n type ($n_s = 1.1 \times 10^{14} \text{ cm}^{-2}$ at 300 K). In previous reports of ferromagnetic ordering in single phase LT-(Ga,Mn)As, the observation of EHE has been attributed to spin-polarized carriers that mediate ferromagnetic ordering between localized spins.²⁷ ac Hall measurements for samples A–C are plotted in Fig. 1(d), and the behavior is consistent with previously reported LT-(Ga,Mn)As with onset of non-linear Hall response below ~ 280 K. Further details of the magnetotransport measurements will be presented elsewhere.

From the transport measurements, it is highly probable that significant levels of the implanted species are electrically active at room temperature and that for all samples, implantation damage dominates transport properties (show insulatorlike behavior) except that of Mn implanted p^+ GaAs:C, which shows changes in slope as reported in LT-(Ga,Mn)As samples, in which anomalies coincide near

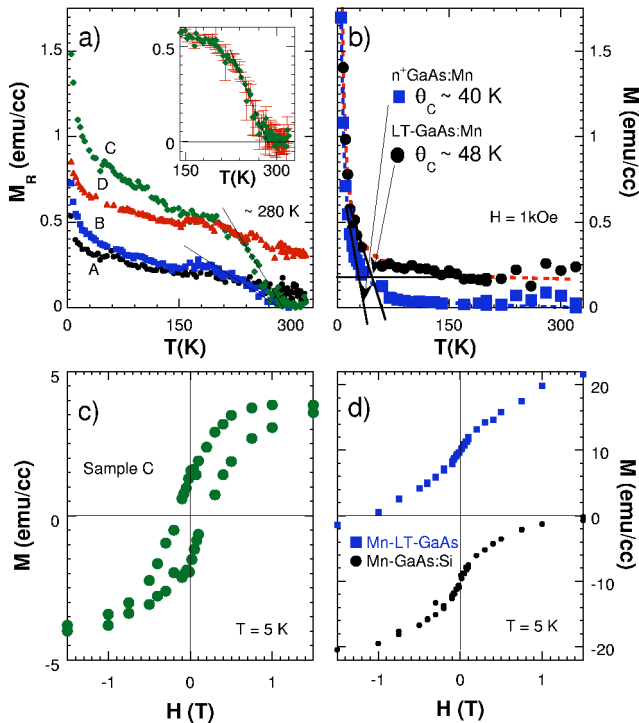


FIG. 2. (Color online) (a) M_R as a function of temperature (T) for Mn implanted p^+ GaAs:C (near T_C for sample C, inset). (b) Magnetization (M) as a function of T for samples X and Y with Curie-Weiss Law fit. M as a function of applied field at 5 K for sample C (c) and samples X and Y, offset for clarity (d).

the magnetic transition temperatures. This feature is absent in ion-implanted LT-GaAs and n^+ GaAs:Si samples. Although Theodoropoulou *et al.* report of unconventional carrier-mediated ferromagnetism in ion-implanted (Ga,Mn)P:C.²⁸ They showed a distinct difference in magnetic properties between Mn ion-implanted GaP:C and n -GaP, consistent with hole mediated ferromagnetic ordering in III-V DMS.

The magnetic properties of Mn implanted GaAs:C, LT-GaAs, and GaAs:Si was measured using the Quantum Design Magnetic Property Measurement System (MPMS). Figure 2(a) plots the remanent magnetization (M_R) as a function of temperature for samples A–D. Magnetic field of 5 T was applied at 5 K and switched off, followed by series of magnetization measurements at zero applied field and at various temperatures (up to 320 K). For samples A–C, nonzero M_R was found for temperatures below ~ 280 K. Unlike LT-(Ga,Mn)As, T_C 's of samples A–C are weakly dependent on Mn content, to be discussed later. Similar measurement of samples X and Y show a near zero flat response indicating paramagneticlike behavior, which is confirmed by magnetic hysteresis measurements at 5 K with near zero M_R [Fig. 2(d)]. Magnetization as a function of temperature (M vs T) measurements with applied field of 1000 Oe show Curie-Weiss temperatures (θ_C) below ~ 50 K for samples X and Y [Fig. 2(b)], which is confirmed by equal traces for zero field cooled and field cooled measurement with a read field of 100 Oe from 5–300 K. The B - H loops for p^+ GaAs:C implanted samples show well-defined magnetic hysteresis loops with

high M_R compared to GaAs:Si and LT-GaAs implanted samples [Figs. 2(c), 2(d)].

As reported for LT-(Ga,Mn)As samples on the insulator side of metal-insulator transition, complete magnetic saturation in samples A–C was found to be difficult; thus, calculation of magnetic moment per Mn atom would yield incomplete values. For sample C, at 5 K and at M_R , we approximate less than $\sim 1/10$ of the implanted Mn to magnetically contribute, assuming Mn spin $S = 5/2$ and the Landé factor $g_{Mn} = 2$. From B - H loops of p^+ GaAs:C implanted samples, we found the coercive field (H_C) to range from few hundred Oe to 2000 Oe with maximum coercive field measured from sample C. A similar trend for approximate magnetic saturation (M_S) was found with maximum $\sim M_S$ corresponding to sample C with Mn dose of 3×10^{16} cm $^{-2}$.

The weak dependence of T_C to Mn dose may suggest an inhomogeneous profile (i.e., equal peak concentration at some distance from surface for samples A–C). As depth profile AES showed a near constant Mn concentration, we note that p is greater than the effective magnetic impurity concentration ($x_{\text{eff}}N_0$) for samples A–C unlike LT-(Ga,Mn)As where p is less than Mn concentration. In their study of carrier-induced ferromagnetism in p -ZnMnTe, Ferrand *et al.* propose for the case where $p > x_{\text{eff}}N_0$ that the Rudermann-Kittel-Kasuya-Yosida (RKKY) model best describes the ferromagnetic ordering since the Zener model ceases to be valid.³¹ In such a view, the weak dependence of T_C on implanted dose may be explained as the tendency of T_C to increase with $x_{\text{eff}}N_0$ being offset Mn-Mn interactions as p increases in this RKKY regime ($p > x_{\text{eff}}N_0$).

Again, without the observed unexpected differences in magnetic properties of Mn implanted p^+ GaAs:C samples with n^+ GaAs:Si and LT-GaAs implanted samples, observed magnetic properties, including possibly the observed weak dependence of T_C to Mn implantation does, might be easily assigned to intermetallic ferromagnetic precipitates such as MnAs, GaMn, and Ga-Mn-As. For the samples considered, sample X would be most susceptible to formation of ferromagnetic precipitates with well-known excess of As in LT-GaAs. In their careful study of different possible secondary phases, Moreno *et al.* have identified three possible precipitates: hexagonal MnAs, zinc blende Mn(Ga)As, and MnGa.²² For samples A–C, ion implanted p^+ GaAs:C samples, the T_C and magnetization values measured do not correspond to the mentioned precipitates as well as Mn₃GaC (T_C of ~ 250 K), to be detailed later.²⁹ From M_R as a function of temperature trace, sample D behavior of apparent T_C greater than 320 K points to formation of MnGa ($T_C > 400$ K) precipitates in agreement with Moreno *et al.* and Shi *et al.*³⁰ The magnetic properties of samples A–C corroborate our findings from HRXRD measurements.

In comparing the magnetic properties of samples A–C with Mn ion-implanted samples X and Y, it is evident that high hole carrier concentrations mediate ferromagnetic ordering between localized spins. Whether these localized spins are associated with substitutional Mn²⁺ ions or a physically undetected intermetallic ferromagnetic clusters, there is a strong evidence that free carrier concentration play an important role in mediating this ferromagnetic ordering,

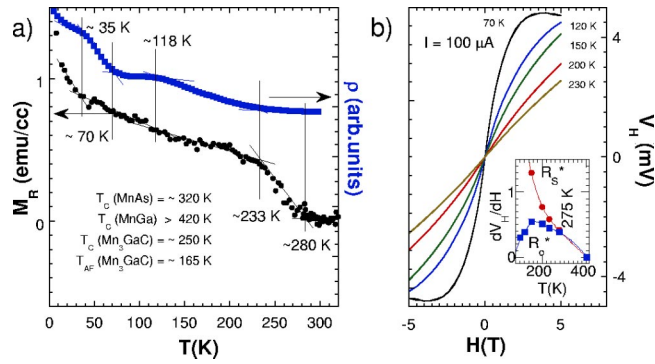


FIG. 3. (Color online) (a) M_R and ac resistivity ($I = 100 \mu\text{A}$) as a function of temperature for sample C ($T_C \sim 280$ K) at $H = 0$. Anomalies in transport properties correspond to magnetic properties suggesting changes in resistivity are due to magnetic ordering in the sample. (b) ac-Hall measurement at various temperature for sample C. Inset shows low field and high field fit to the Hall response corresponding to ordinary and extraordinary Hall coefficient for sample C, indicating nonlinear Hall response below ~ 275 K.

evident in increased M_R and T_C , especially comparing carbon doped GaAs implanted samples (A–C) to LT-GaAs and Si doped GaAs samples (X and Y). From physical characterization studies, we did not observe any secondary phases or trends observed by others studying intermetallic clusters in semiconductor matrix for all samples except with highest Mn dose (sample D). In addition, if secondary ferromagnetic phases created by the implanted ions were responsible for the observed magnetic properties, then we expect similar results in Mn ion-implanted carbon doped p^+ GaAs as well as in LT-GaAs and Si doped n^+ GaAs, as formation of such physically undetected ferromagnetic phases as MnAs, GaMn, and Mn(Ga)As would be, at the least, equally probable in all samples considered. For possible undetected ferromagnetic phases unique to carbon doped samples, Mn₃GaC with ferromagnetic transition temperature ~ 250 K is a possibility, but this perovskite-type material has a well known antiferromagnetic transition at ~ 165 K at zero magnetic field, which should have been clearly evident from the M_R vs T measurements as well as M vs H measurements at 5 K.²⁹ From transport measurements, we observed characteristic anomalies corresponding to magnetic properties as well as the EHE (Fig. 3), a telling sign that the carriers are spin polarized and

mediate ferromagnetic ordering between localized spins. Plotting Hall effect response (dV_H/dH) at high fields [directly proportional to the ordinary Hall effect coefficient (R_0)] and at low fields [EHE coefficient (R_S)], we observe a distinct difference near T_C observed from temperature dependence of M_R [Fig. 3(b), inset].

To summarize, we have observed remanent magnetization up to ~ 280 K for Mn ion-implanted p^+ GaAs:C. From physical property measurements, we cannot attribute the magnetic properties to an observed presence of secondary ferromagnetic phases such as MnAs, Mn(Ga)As, Mn₃GaC, and GaMn. This result is supported by magnetic properties of LT-GaAs and n^+ GaAs:Si Mn ion-implanted (under same conditions) samples, which show neither the marked increase in magnetic ordering temperatures and remanent magnetization nor magnetic properties that can be attributed to physically undetected ferromagnetic secondary phases. This difference between samples (Mn implanted carbon doped p^+ GaAs vs Mn implanted LT-GaAs and Si doped n^+ GaAs) points to a role of the carbon acceptor impurity, which substitutionally prefers the group V (or As) site and provide hole carriers. Whether this role of carbon acceptor in the observation of increased magnetic properties is due to increased number of free carrier concentration or due to a secondary ferromagnetic phase unique to carbon (Mn₃GaC) arguably cannot be currently irrefutably answered in detail. But, such properties as antiferromagnetic transition attributable to Mn₃GaC were not observed. Transport measurements of Mn ion-implanted p^+ GaAs:C samples do not agree with results as reported by others of nanometer-sized ferromagnetic clusters embedded in semiconductor matrix. Rather transport measurements correspond with temperature dependence of magnetic properties, very similar to LT-(Ga,Mn)As. Additionally, observation of nonlinear Hall response (or EHE) corresponds to observed magnetic ordering temperature.

We would like to thank Dr. J. Chang of KIST with the TEM analysis and Drs. H.C. Kim and S.-H. Park of KBSI Material Science Laboratory with access to PPMS. The work at SNU was supported by KOSEF and Samsung Electronics Endowment through CSCMR. The work at UF was supported by NSF Grant Nos. DMR0101438 and ECS 02242303 and by ARO under Grant No. DAAD 190110701 and 19021420.

*Electronic address: parkyd@phy.snu.ac.kr

¹H. Munekata, H. Ohno, S. von Molnar, Armin Segmüller, L.L. Chang, and L. Esaki, Phys. Rev. Lett. **63**, 1849 (1989).

²J. De Boeck, R. Oesterholt, A. Van Esch, H. Bender, C. Bruynseraede, C. Van Hoof, and G. Borghs, Appl. Phys. Lett. **68**, 2744 (1996); H. Ohno, A. Shen, F. Matsukura, A. Oiwa, A. Endo, S. Katsumoto, and Y. Iye, *ibid.* **69**, 363 (1996).

³S.A. Wolf, D.D. Awschalom, R.A. Buhrman, J.M. Daughton, S. von Molnar, M.L. Roukes, A.Y. Chtchelkanova, and D.M. Treger, Science **294**, 1488 (2001).

⁴T. Hayashi, Y. Hashimoto, S. Katsumoto, and Y. Iye, Appl. Phys. Lett. **78**, 1691 (2001).

⁵K.C. Ku, S.J. Potashnik, R.F. Wang, S.H. Chun, P. Schiffer, N.

Samarth, M.J. Seong, A. Mascarenhas, E. Johnston-Halperin, R.C. Myers, A.C. Gossard, and D.D. Awschalom, Appl. Phys. Lett. **82**, 2302 (2003); S.J. Potashnik, K.C. Ku, S.H. Chun, J.J. Berry, N. Samarth, and P. Schiffer, *ibid.* **79**, 1495 (2001).

⁶K.W. Edmonds, K.Y. Wang, R.P. Campion, A.C. Neumann, N.R.S. Farley, B.L. Gallagher, and C.T. Foxon, Appl. Phys. Lett. **81**, 4991 (2002).

⁷M. Berciu and R.N. Bhatt, Phys. Rev. Lett. **87**, 107203 (2001); R.N. Bhatt, M. Berciu, M.P. Kennett, and Xin Wan, J. Supercond. **15**, 71 (2002).

⁸A. Kaminski and S. Das Sarma, Phys. Rev. Lett. **88**, 247202 (2002).

⁹P.A. Korzhavyi, I.A. Abrikosov, E.A. Smirnova, L. Bergqvist, P.

- Mohn, R. Mathieu, P. Svedlindh, J. Sadowski, E.I. Isaev, Yu.Kh. Vekilov, and O. Eriksson, *Phys. Rev. Lett.* **88**, 187202 (2002).
- ¹⁰T. Jungwirth, J. König, J. Sinova, J. Kuačera, and A.H. MacDonald, *Phys. Rev. B* **66**, 012402 (2002).
- ¹¹H. Ohno, *J. Magn. Magn. Mater.* **200**, 110 (1999).
- ¹²H. Ohldag, V. Solinus, F.U. Hillebrecht, J.B. Goedkoop, M. Finazzi, F. Matsukura, and H. Ohno, *Appl. Phys. Lett.* **76**, 2928 (2000).
- ¹³Y. Satoh, D. Okazawa, A. Nagashima, and J. Yoshino, *Physica E* **10**, 196 (2001).
- ¹⁴H. Ohno, D. Chiba, F. Matsukura, T. Omiya, E. Abe, T. Dietl, Y. Ohno, and K. Ohtani, *Nature (London)* **408**, 944 (2000).
- ¹⁵Y.D. Park, A.T. Hanbicki, S.C. Erwin, C.S. Hellberg, J.M. Sullivan, J.E. Mattson, T.F. Ambrose, A. Wilson, G. Spanos, and B.T. Jonker, *Science* **295**, 651 (2002).
- ¹⁶C.R. Abernathy, F. Ren, P.W. Wisk, S.J. Pearton, and E. Esagui, *Appl. Phys. Lett.* **61**, 1092 (1992).
- ¹⁷W. Li and M. Pessa, *Phys. Rev. B* **57**, 14 627 (1998).
- ¹⁸E.F. Schubert, G.H. Gilmer, R.F. Kopf, and H.S. Luftman, *Phys. Rev. B* **46**, 15 078 (1992).
- ¹⁹C.R. Abernathy, *Mater. Sci. Eng., R.* **14**, 203 (1995).
- ²⁰S.J. Pearton, C.R. Abernathy, M.E. Overberg, G.T. Thaler, D.P. Norton, N. Theodoropoulou, A.F. Hebard, Y.D. Park, F. Ren, J. Kim, and L.A. Boatner, *J. Appl. Phys.* **93**, 1 (2003); S.J. Pearton, C.R. Abernathy, D.P. Norton, A.F. Hebard, Y.D. Park, L.A. Boatner, and J.D. Budai, *Mater. Sci. Eng., R.* **286**, 1 (2003).
- ²¹M.A. Scarpulla, O.D. Dubon, K.M. Yu, O. Monteiro, M.R. Pillai, M.J. Aziz, and M.C. Ridgway, *Appl. Phys. Lett.* **82**, 1251 (2003).
- ²²M. Moreno, A. Trampert, B. Jenichen, L. Däweritz, and K.H. Ploog, *J. Appl. Phys.* **92**, 4672 (2002).
- ²³H. Akinaga, J. De Boeck, G. Borghs, S. Miyanishi, A. Asamitsu, W. Van Roy, Y. Tomioka, and L.H. Kuo, *Appl. Phys. Lett.* **72**, 3368 (1998).
- ²⁴D.R. Schmidt, A.G. Petukhov, M. Foygel, J.P. Ibbetson, and S.J. Allen, *Phys. Rev. Lett.* **82**, 823 (1999).
- ²⁵Y.D. Park, A. Wilson, A.T. Hanbicki, J.E. Mattson, T. Ambrose, G. Spanos, and B.T. Jonker, *Appl. Phys. Lett.* **78**, 2739 (2001).
- ²⁶Y. Iye, A. Oiwa, A. Endo, S. Katsumoto, F. Matsukura, A. Shen, H. Ohno, and H. Munekata, *Mater. Sci. Eng., B* **63**, 88 (1999).
- ²⁷T. Jungwirth, Qian Niu, and A.H. MacDonald, *Phys. Rev. Lett.* **88**, 207208 (2002).
- ²⁸N. Theodoropoulou, A.F. Hebard, M.E. Overberg, C.R. Abernathy, S.J. Pearton, S.N.G. Chu, and R.G. Wilson, *Phys. Rev. Lett.* **89**, 107203 (2002).
- ²⁹J-P. Bouchaud, R. Fruchart, R. Pauthenet, M. Guillot, H. Bartholin, and F. Chaisé, *J. Appl. Phys.* **37**, 971 (1966); T. Kanomata, M. Kikuchi, T. Kaneko, K. Kamishima, M.I. Bartashevich, H.A. Katori, and T. Goto, *Solid State Commun.* **101**, 811 (1997).
- ³⁰J. Shi, J.M. Kikkawa, D.D. Awschalom, G. Medeiros-Ribeiro, P.M. Petroff, and K. Babcock, *J. Appl. Phys.* **79**, 5296 (1996).
- ³¹D. Ferrand, J. Cibert, A. Wasiela, C. Bourgognon, S. Tatarenko, G. Fishman, T. Andrearczyk, J. Jaroszyński, S. Koleśnik, T. Dietl, B. Barbara, and D. Dufeu, *Phys. Rev. B* **63**, 085201 (2001).